

Ultraviolet light emission and excitonic fine structures in ultrathin single-crystalline indium oxide nanowires

Z. P. Wei,¹ D. L. Guo,¹ B. Liu,¹ R. Chen,¹ L. M. Wong,² W. F. Yang,¹ S. J. Wang,² H. D. Sun,^{1,a)} and T. Wu^{1,b)}

¹*Division of Physics and Applied Physics, School of Physical and Mathematical Sciences, Nanyang Technological University, Singapore 637371, Singapore*

²*Institute of Materials Research and Engineering, Singapore 117602, Singapore*

(Received 19 November 2009; accepted 11 December 2009; published online 19 January 2010)

We report the ultraviolet light emission from ultrathin indium oxide (In_2O_3) nanowires fabricated by the vapor-liquid-solid method. The high crystalline quality of the samples is confirmed by using x-ray diffraction, scanning electron microscopy, and transmission electron microscopy. Strong ultraviolet light emission is consistently observed in the temperature dependent photoluminescence measurements carried out between 10 and 300 K. Emissions related to free excitons and bound exciton complexes, donor-acceptor pair transition and its relevant longitudinal optical phonon replicas are identified and their temperature-dependent evolution is discussed in details. © 2010 American Institute of Physics. [doi:10.1063/1.3284654]

In recent years, there has been intensive research on low-dimensional nanomaterials because of their unique physical properties and potential applications in nanoelectronics and nanophotonics.^{1–5} Indium oxide (In_2O_3) is a very important wide band gap (3.50–3.75 eV) semiconductor,^{6,7} which has been widely used as a transparent conductor in window heaters, solar cells, and flat-panel displays.⁸ In_2O_3 has the bixbyite structure, being body-centered cubic with space group $I213$,⁹ and $a=1.011$ nm. Over the past few years, there have been an increasing number of reports on the synthesis of In_2O_3 nanostructures via various routes such as vapor-solid method, laser ablation process, vapor-liquid-solid (VLS) technique, and so on.^{10–12} However, most of the effort has focused on optimizing the material fabrication and exploring the electrical properties, while the optical properties of In_2O_3 nanostructures, especially their light emission characteristics, have been rarely investigated.

Although bulk In_2O_3 does not emit light at room temperature, there have been recent reports on the blue-green photoluminescence (PL) in thin films, nanoparticles, and nanowires.^{13–18} These reports suggested that the broad light emission peaked in the range of 400–650 nm can be attributed to the high-density oxygen vacancies, thus referred as deep-level or trap-state emissions.^{15,16,18} However, large discrepancies exist in the literatures regarding the emission characteristics because they originate from the incomplete oxidation during the materials synthesis, which may varies in different experiments. Up till now ultraviolet (UV) emission in In_2O_3 has been sparsely documented.^{19,20} In a very recent report, a UV emission peaked at 378 nm (~ 3.28 eV) with a narrow FWHM of 13 nm was observed in vertical In_2O_3 nanowires grown on a-plane sapphire substrates.²⁰ Although these reports are encouraging, the lack of systematic study on the low temperature PL properties of In_2O_3 prevents a clear understanding on the emission mechanisms and the excitonic characteristics.

In this letter, high crystalline quality In_2O_3 nanowires were fabricated via a VLS route and their optical properties have been investigated in details by temperature dependent and excitation-power dependent PL experiments. Rich fine structures in the UV region of the PL spectra have been observed, and systematic analysis allow us to assign these fine structures to the recombination of free exciton (FX), bound exciton complexes (BECs), and donor-acceptor pairs (DAP).

In_2O_3 nanowire samples were prepared on silicon substrates (with ~ 4 nm Au catalyst) via a vapor transport growth route similar to our previous reports on the growth of high quality oxide nanowires.^{21,22} In_2O_3 /graphite powder with a 2:3 weight ratio was used as the source. Growth took place at 900° C with argon containing 0.05% oxygen as the carrying gas. The structure and morphology of the samples were determined by x-ray powder diffraction (XRD), scanning electron microscopy (SEM), and transmission electron microscopy (TEM). For PL measurements, the 325 nm line from a He-Cd laser was used as the excitation source. The PL signal was dispersed by a 750 mm monochromator and collected by a photo multiplier tube in a backscattering geometry using the standard lock-in technique.

The XRD pattern of the as-grown In_2O_3 nanowires was shown in Fig. 1(a). All of the diffraction peaks can be indexed as the bixbyite In_2O_3 structure ($a=1.011$ nm), which is consistent with the JCPDS file No. 89–4595. This indicates that the nanowires are composed of pure In_2O_3 . Figures 1(b) and 1(c) are the low magnification and the cross-sectional SEM images of the In_2O_3 nanowires, respectively. The nanowires cover the surface of the substrate uniformly. They are 1 μm in length and 20–40 nm in diameter, and the Au catalyst particles on the top of nanowires can be clearly seen. Figure 1(d) shows the high resolution TEM image of a single In_2O_3 nanowire. The lattice spacing of 0.255 nm is corresponding to the (400) planes of In_2O_3 , indicating that the nanowires grow along $\langle 100 \rangle$. Low resolution TEM image and energy dispersive x-ray spectroscopy (EDS) element mappings of In, O, and Au were taken on an individual nanowire [Figs. 1(e) and 1(h)]. It can be seen that the nanowire is

^{a)}Electronic mail: hdsun@ntu.edu.sg.

^{b)}Electronic mail: tomwu@ntu.edu.sg.

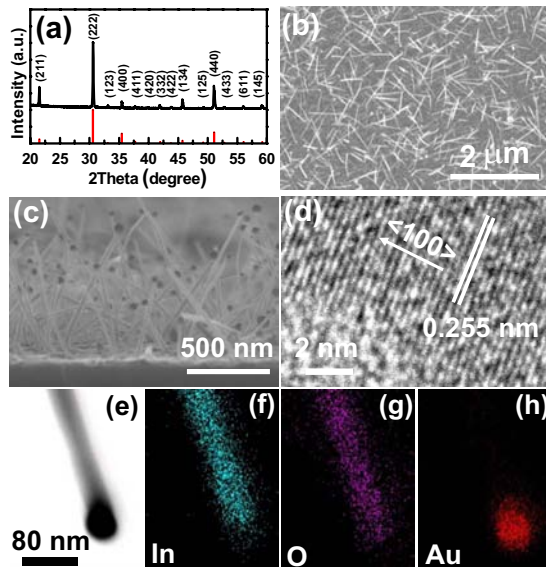


FIG. 1. (Color online) (a) XRD pattern of In_2O_3 nanowires. The powder diffraction data (JCPDS Card No. 89-4595) is also shown. (b) Typical SEM image of the as-synthesized nanowires. (c) Cross-sectional SEM image of In_2O_3 nanowires. (d) High-resolution TEM image of a single In_2O_3 nanowire. [(e)–(h)] Low resolution TEM image and EDS element mappings of In, O, and Au.

composed of indium and oxygen with a gold nanoparticle on the top.

Figure 2(a) shows the PL spectrum of In_2O_3 nanowires in an extended wavelength range taken at 10 K. Besides the prominent UV emission, a broad emission band is located at ~ 2.450 eV. This deep level emission band is believed to originate from the crystal defects, e.g., oxygen vacancies in the nanowires.¹⁸ Its much lower intensity compared to the UV emission indicates the very high crystalline quality of the sample. It is interesting to note that this defect-related emission band has a fine structure with a fixed energy separation of 72 meV, which is close to the phonon energy of In_2O_3 .²³

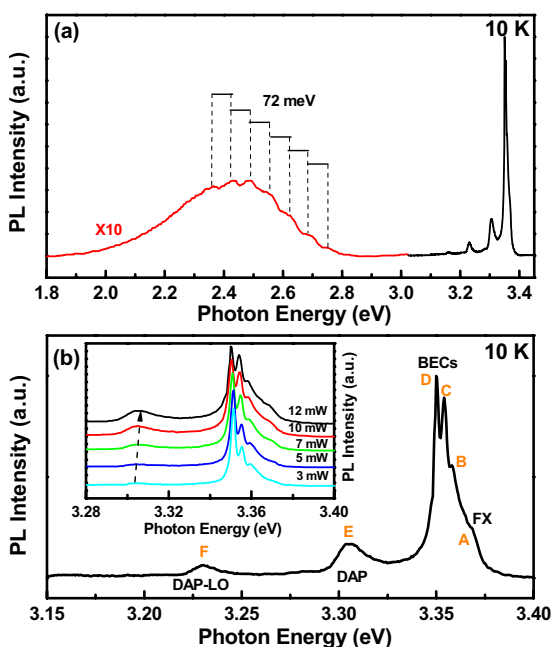


FIG. 2. (Color online) (a) PL spectrum of In_2O_3 nanowires measured at 10 K. (b) High resolution PL spectrum of the sample in the UV regime. The inset is the excitation-power dependent PL spectra of In_2O_3 nanowires at 10 K.

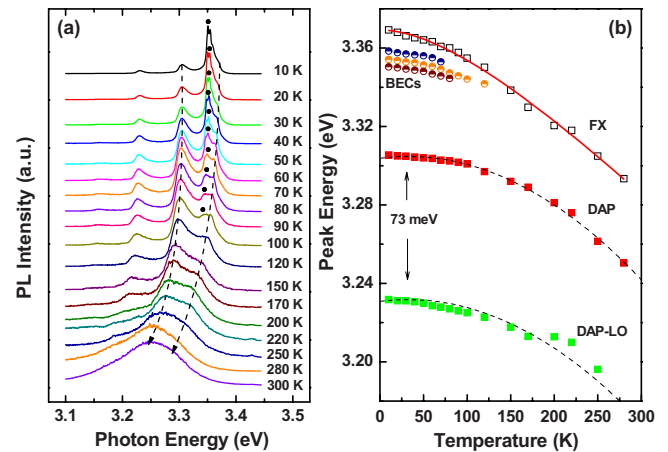


FIG. 3. (Color online) (a) Temperature dependent PL spectra from 10 to 300 K. (b) The temperature dependence of the peak positions. The solid line is the fitting curve of the experimental data according to the Varshni equation. The dashed lines are guide to the eyes.

Although there has been no report on this feature in In_2O_3 so far, an analogous feature has been observed in ZnO ,²⁴ which indicates a very strong electron-phonon interaction in the material.

Let's focus our discussion on the UV emission depicted in Fig. 2(b), which is the dominant feature of the spectrum. The UV emission consists of six distinct peaks at 3.369, 3.359, 3.354, 3.350, 3.305, and 3.232 eV, which were labeled as peaks A-F, respectively. Such fine features in the UV regime have not been reported so far. We assign the peak A to FX, and the peaks B, C, and D to BECs, which we will discuss below in details. The peaks E and F are related to the recombination of DAP and its first-order longitudinal optical (LO)-phonon replica, respectively. This assignment was evidenced by the excitation-power dependent PL measurement which is shown in the inset of Fig. 2(b). The energy of DAP luminescence can be expressed as: $E_g - E_D - E_A + e^2/4\pi\epsilon r$, where E_g is the band gap energy, E_D and E_A are the donor and acceptor binding energy, e is the elementary electric charge, ϵ is the dielectric constant, and r is the donor-acceptor pair distance. With increased excitation power, the density of photon excited DAP becomes higher, leading to the decrease in the DAP distance. Thus, the DAP peak exhibits a blueshift when the laser power density is increased, or smaller r , which in turn increases the DAP energy. This was confirmed in our data—the DAP band exhibits a 3 meV blueshift as the excitation power increases from 3 to 12 mW. The energy spacing between the peak F and the DAP emission (peak E) is 73 meV, which is close to the phonon energy involved in the deep level emission as shown in Fig. 2(a), and therefore peak F can be attributed to the first-order LO phonon replica of DAP (DAP-1LO). In the Franck-Condon model, the coupling strength between the radiative transition and the LO-phonon can be characterized by the Huang-Rhys factor S .^{25,26} The relative intensity of the n th phonon replica I_n is related to the zero-phonon peak I_0 by the S factor as $I_n = I_0(S^n e^{-S}/n!)$, where n is a natural number. From the measured spectrum, the S factor associated with DAP is estimated to be 0.25.

Figure 3(a) shows the temperature dependent PL spectra taken on the sample between 10 and 300 K. The intensity of peaks B, C, and D, which are labeled by dots, decreases very quickly with increasing temperature and cannot be resolved

at temperatures higher than 100 K. At the same time, peak A which appears as the higher energy shoulder at 3.369 eV becomes more and more pronounced at higher temperatures. This characteristic is very similar to the emission transformation from bound exciton, or BECs, to FX. As the temperature increases, the bound excitons have enough thermal energy to dissociate and become FX, which is a well-known phenomenon for wide band gap semiconductors like ZnO.²⁷ However, it has not been reported for In₂O₃ so far presumably due to the lack of low temperature PL studies on high quality samples. The excitation power dependent PL data also supports assigning peaks B, C, and D as BECs because their peak energy exhibits a slight red shift which is probably due to the heating effect under the high excited power, as observed in other semiconductors.²⁸ At temperatures higher than 100 K, the PL spectra of In₂O₃ nanowires are mainly composed of FX and DAP emissions. At room temperature, the PL peak is dominated by the DAP emission at 3.265 eV, which is accompanied by the FX emission appearing as a higher energy shoulder around 3.290 eV. This result corroborates the data of 3.280 eV (378 nm) previously reported on In₂O₃ nanowires.²⁰

The temperature dependence of the peak energies of the peaks is shown in Fig. 3(b). The dashed lines through DAP and its LO phonon replica are guide to the eyes. It clearly shows that the energy difference between DAP and its LO-phonon replica is well defined to be 73 meV in the whole range of measurement temperature. This further confirms the previous assignment. The FX peak energy decreases monotonically with increasing temperature, which can be well described by the empirical Varshni equation,^{29,30}

$$E(T) = E(0) - \frac{\alpha T^2}{T + \beta}, \quad (1)$$

where $E(0)$ is the excitonic band gap at 0 K, and α and β are the corresponding thermal coefficients. The open squares in Fig. 3(b) are the experimental data of FX peak energy and the red line is the fitting curve obtained by using the Varshni's equation. It is clearly shown that the curve fits our experimental data very well. The value of $E(0)$ obtained from the fitting is 3.370 eV, with $\alpha = 4.7 \times 10^{-4}$ eV/K and $\beta = 205.5$ K. The value of the band gap in In₂O₃ and its direct/indirect nature are still under intensive discussion. The reported data in the previous literatures range from 3.50 to 3.75 eV.^{6,7} $E(0)$ of 3.370 eV should be taken as the lower bound of the band gap due to the finite exciton binding energy of In₂O₃. Our results call for more in-depth investigations on the physical properties of high-quality In₂O₃ samples to determine the associated band structure.

In summary, high quality In₂O₃ nanowires have been fabricated by using the VLS growth method, and characterized by XRD, SEM, and TEM. Through high resolution PL measurements, we have observed rich fine structures in the UV regime. The recombination of FX, bound exciton complexes, DAP, and their LO replicas have been identified by detailed analysis of the temperature- and excitation intensity-

dependent PL spectra. Such high quality In₂O₃ nanowires may help to shed light on its electronic band structures and find application in photonic and light emitting devices.

This work is supported by the Singapore National Research Foundation (Grant No. RCA-08/018), and MOE Grant No. RG40/07. The author (Z.P.W.) acknowledges the support under Project of Science Development Planning and Department of Education of Jilin Province under Grant Nos. 20090139, 20070519, 20080296, and 20080297.

¹A. M. Morales and C. M. Lieber, *Science* **279**, 208 (1998).

²L. E. Greene, M. Law, D. H. Tan, M. Montano, J. Goldberger, G. Somorjai, and P. D. Yang, *Nano Lett.* **5**, 1231 (2005).

³L. Vayssieres, *Adv. Mater.* **15**, 464 (2003).

⁴Y. N. Xia, P. D. Yang, Y. G. Sun, Y. Y. Wu, B. Mayers, B. Gates, Y. D. Yin, F. Kim, and Y. Q. Yan, *Adv. Mater.* **15**, 353 (2003).

⁵D. P. Yu, Z. G. Bai, Y. Ding, Q. L. Hang, H. Z. Zhang, J. J. Wang, Y. H. Zou, W. Qian, G. C. Xiong, H. T. Zhou, and S. Q. Feng, *Appl. Phys. Lett.* **72**, 3458 (1998).

⁶F. Matino, L. Persano, V. Arima, D. Pisignano, R. I. R. Blyth, R. Cingolani, and R. Rinaldi, *Phys. Rev. B* **72**, 085437 (2005).

⁷A. Walsh, J. L. F. Da Silva, S. H. Wei, C. Korber, A. Klein, L. F. J. Piper, A. DeMasi, K. E. Smith, G. Panaccione, P. Torelli, D. J. Payne, A. Bourlange, and R. G. Egdell, *Phys. Rev. Lett.* **100**, 167402 (2008).

⁸I. Hamberg and C. G. Granqvist, *J. Appl. Phys.* **60**, R123 (1986).

⁹M. Marezio, *Acta Crystallogr.* **20**, 723 (1966).

¹⁰X. S. Peng, G. W. Meng, J. Zhang, X. F. Wang, Y. W. Wang, C. Z. Wang, and L. D. Zhang, *J. Mater. Chem.* **12**, 1602 (2002).

¹¹X. C. Wu, J. M. Hong, Z. J. Han, and Y. R. Tao, *Chem. Phys. Lett.* **373**, 28 (2003).

¹²D. H. Zhang, C. Li, S. Han, X. L. Liu, T. Tang, W. Jin, and C. W. Zhou, *Appl. Phys. Lett.* **82**, 112 (2003).

¹³K. C. Kam, F. L. Deepak, A. K. Cheetham, and C. N. R. Rao, *Chem. Phys. Lett.* **397**, 329 (2004).

¹⁴M. S. Lee, W. C. Choi, E. K. Kim, C. K. Kim, and S. K. Min, *Thin Solid Films* **279**, 1 (1996).

¹⁵C. H. Liang, G. W. Meng, Y. Lei, F. Phillipp, and L. D. Zhang, *Adv. Mater.* **13**, 1330 (2001).

¹⁶X. P. Shen, H. J. Liu, X. Fan, Y. Jiang, J. M. Hong, and Z. Xu, *J. Cryst. Growth* **276**, 471 (2005).

¹⁷C. Q. Wang, D. R. Chen, X. L. Jiao, and C. L. Chen, *J. Phys. Chem. C* **111**, 13398 (2007).

¹⁸H. J. Zhou, W. P. Cai, and L. D. Zhang, *Appl. Phys. Lett.* **75**, 495 (1999).

¹⁹H. Q. Cao, X. Q. Qiu, Y. Liang, Q. M. Zhu, and M. J. Zhao, *Appl. Phys. Lett.* **83**, 761 (2003).

²⁰C. J. Chen, W. L. Xu, and M. Y. Chern, *Adv. Mater.* **19**, 3012 (2007).

²¹G. Z. Xing, J. B. Yi, J. G. Tao, T. Liu, L. M. Wong, Z. Zhang, G. P. Li, S. J. Wang, J. Ding, T. C. Sum, C. H. A. Huan, and T. Wu, *Adv. Mater.* **20**, 3521 (2008).

²²Z. Zhang, J. Gao, L. M. Wong, J. G. Tao, L. Liao, Z. Zheng, G. Z. Xing, H. Y. Peng, T. Yu, Z. X. Shen, C. H. A. Huan, S. J. Wang, and T. Wu, *Nanotechnology* **20**, 135605 (2009).

²³R. L. Weiher and R. P. Ley, *J. Appl. Phys.* **37**, 299 (1966).

²⁴R. Dingle, *Phys. Rev. Lett.* **23**, 579 (1969).

²⁵Y. Toyozawa and J. Hermanson, *Phys. Rev. Lett.* **21**, 1637 (1968).

²⁶R. Chen, G. Z. Xing, J. Gao, Z. Zhang, T. Wu, and H. D. Sun, *Appl. Phys. Lett.* **95**, 061908 (2009).

²⁷U. Ozgur, Y. I. Alivov, C. Liu, A. Teke, M. A. Reshchikov, S. Dogan, V. Avrutin, S. J. Cho, and H. Morkoc, *J. Appl. Phys.* **98**, 041301 (2005).

²⁸D. C. Reynolds, D. C. Look, and B. Jogai, *J. Appl. Phys.* **88**, 5760 (2000).

²⁹Y. P. Varshni, *Physica* **34**, 149 (1967).

³⁰H. W. Suh, G. Y. Kim, Y. S. Jung, W. K. Choi, and D. Byun, *J. Appl. Phys.* **97**, 044305 (2005).